

## Ion Drag EHD Micropump with Single Walled Carbon Nanotube (SWCNT) Electrodes

Md. Kamrul RUSSEL, P. Ravi SELVAGANAPATHY, Chan Y. CHING\*

\* Corresponding author: Tel.: +1 905 525 9140; Fax: +1 905 572 7944; Email: chingcy@mcmaster.ca (Chan Y. CHING)

Department of Mechanical Engineering, McMaster University, Canada

**Abstract** Ion drag electrohydrodynamic (EHD) micropumps are promising in a number of micro-scale applications due to its small form factor, low power consumption, ability to work with dielectric heat transfer fluids, good controllability and absence of any moving parts. Ion drag EHD micro-pumps have been studied widely and the pressure head has been reported to depend on electrode material (i.e., work function), geometric configuration, electrode surface topology and applied electric field. One drawback of such pumps is the relatively low pressure head generation and high threshold voltage required for the onset of charge injection for practical applications. The presence of micro/nano features with sharp asperities on the emitter electrodes is likely to enhance the local electric field and charge injection significantly and thus, the pressure generation. The objective of this work is to investigate the effect of surface topology on the charge injection and pressure generation in HFE 7100. Experiments were performed using micropumps with smooth and single wall carbon nanotube (SWCNT) deposited on smooth gold electrodes. A lower threshold voltage, higher charge injection and pressure head was found for the micropump with SWCNT deposited on smooth electrodes compared to the no deposition case.

**Keywords:** Micro Pump, SWCNT, Pressure Head

### 1. Introduction

Thermal management in electronic devices is becoming increasingly challenging due to higher circuit packaging densities. Mudawar [1] broadly identified two ranges of heat fluxes depending on the heat dissipation from the electronic chip: (i) high heat flux ( $10^2 \sim 10^3$  W/cm<sup>2</sup>) and (ii) ultra high heat flux ( $10^3 \sim 10^5$  W/cm<sup>2</sup>) heat dissipation applications. The thermal load most often is also unevenly distributed that can lead to very high local heat densities. Active cooling techniques, such as liquid cooling, have been studied and shown to achieve a cooling capacity up to 1 kW/cm<sup>2</sup> [2]. Microchannel liquid cooling has been studied since Tuckerman and Pease [3] dissipated 790 W/cm<sup>2</sup> using water as the cooling fluid in 50  $\mu$ m x 302  $\mu$ m microchannels. As the effective diameter of the microchannel decreases the

heat dissipation capacity from the chip increases due to the increase in the surface area associated with the cooling fluid over the same footprint of the electric chip. However, the flow resistance in these channels also increases requiring higher external pressure heads to circulate the cooling fluid. A miniaturized pressure source, e.g., micropump integrated within the microchannels, can be used to overcome the resistance to the flow in these microchannels. Among various available micropumps [4], the ion drag EHD micropump is particularly promising due to its small form factor, low power consumption, ability to work with dielectric heat transfer fluids, good controllability and absence of any moving parts.

The principles of ion drag pumping have been known since late 1950's [5]. Since then theoretical [6-9] and experimental [6, 7]

studies have been performed to better understand the pump characteristics. The first injection EHD micropump was fabricated by Richter et al. [10] where two parallel grid electrodes at a spacing of 350  $\mu\text{m}$  were used to achieve a maximum pressure of 2480 Pa at an applied potential of 700 V using ethanol as the working fluid. The first planar electrodes for an ion drag EHD micropump was proposed by Ahn and Kim [11] with an inter electrode spacing of 100  $\mu\text{m}$ . The spacing between each pair of electrodes was 200  $\mu\text{m}$ . A maximum-pressure head and flow rate of 240 Pa and 50  $\mu\text{L}/\text{min}$ , respectively, were reported using ethanol. The effect of fluid [10, 12, 13], microchannel height [14] and electrode design, such as spacing between electrodes and electrode pairs, asymmetry within the two adjacent electrode widths (i.e., 2D asymmetry) and 3D features on the electrodes (e.g., micropillars, microbumps) and their spatial spacing [14-19] on the performance of EHD micropumps have been studied. A higher pumping capacity and lower voltage requirement for the onset of charge injection has been reported when inter-electrode spacing was reduced or asymmetry between the electrodes, both in 2D and 3D, were incorporated.

In general, the EHD pump performance depends on the applied electric field gradient [19] which fundamentally contributes to the charge injection. Charge injection primarily depends on the energy barrier set by the electrode materials, the dielectric liquid and the inter electrode spacing. Asymmetry in an electrode pair (both for 2D and 3D) introduces higher electric field gradients. A higher pressure generation and lower power consumption was reported for the asymmetric electrode configurations when compared to the symmetric electrode pair. One way to further reduce the energy barrier is to lower the work function of the electrode material and thus improve the pump performance. This can be achieved by having sharp features with high aspect ratio such as use of nanotubes/rods on the electrodes [20]. These sharp features not only lower the energy barrier but also introduce fringing electric fields and thus

increase the electric field gradient at their tips. Carvalho [21] showed a reduction factor of 50 in the voltage requirement for the onset of charge injection in air when an electrode surface with vertical copper nanorods (aspect ratio of 300) was compared to a smooth electrode. Similar experiment in a dielectric liquid (HFE 7100) by Russel et al. [22] showed a reduction factor greater than 5 for randomly deposited single walled carbon nanotubes (SWCNT) on the electrodes. In their study, the surface roughness was a secondary effect while the presence of sharp features with high aspect ratio had the primary effect in reducing the voltage required for the onset of the charge injection. In previous studies of 3D asymmetry within the electrodes in an ion drag micropump, the 3D features had an aspect ratio less than one [16, 18, 19]. The features in these studies were not sharp to produce significant enhancement in local electric field gradients.

The objective of this research is to study the effect of sharp features on the EHD pump performance. In particular, SWCNT were deposited onto the planar emitter electrodes of an ion drag EHD micropump to study the required threshold voltage for charge injection, discharge current, pumping head capacity along with corresponding input power requirement using HFE 7100 as the dielectric liquid. These results were compared against the case with no SWCNT. The fabrication of the micropump and experimental methodology is described in the next section, followed by a presentation and discussion of the results. The key conclusions are then finally presented.

## 2. Fabrication and Experimental Methodology

The micropump used in this research was similar to the one studied by Kazemi et al. [17]. The micropumps tested had 100 pairs of electrodes (emitters and collectors) deposited and then lithographically patterned on glass substrate which acts as the bottom wall of a microchannel. The top wall of the microchannel is made of PDMS and then bonded to the glass substrate. The electrodes in

the micropump are of asymmetric planar configuration where the width of the collector electrode was twice that of the emitter electrode (40 and 20  $\mu\text{m}$  respectively). The micropump with its dimensional specifications is shown in Figure 1. Two different pumps were tested with inter electrode spacing,  $d_{ec}$ , of 40 and 120  $\mu\text{m}$  while the spacing between each pair of electrodes was twice the interelectrode spacing, i.e., 80 and 240  $\mu\text{m}$  respectively. The thickness of the electrodes is 0.25  $\mu\text{m}$  while the height and the width of the micro channel were 100  $\mu\text{m}$  and 5 mm respectively. The length of the micro channel depended on the inter electrode spacing ( $d_{ec}$ ) and was 21 and 45 mm for the pumps with  $d_{ec} = 40$  and 120  $\mu\text{m}$  respectively. The details of the fabrication procedures can be found in [17]. SWCNT (1.3-1.5 nm individual diameter and 1-5  $\mu\text{m}$  long, Sigma-Aldrich), prior to the bonding of the PDMS microfluidic channel onto the glass substrate containing the patterned electrodes, was deposited on the emitter electrodes by electrophoretic deposition following the technique proposed by Gao et al. [23]. The SEM images of the electrodes before and after the SWCNTs deposited on them are presented in Figure 2. The electrophoretic method resulted in the deposition of a thin layer of randomly deposited SWCNT on the emitter electrodes of the micropump as shown in the SEM image in Figure 2 (b). The nanotubes remain mostly in horizontal orientation. The SEM image of the smooth electrode (without deposition) is presented in Figure 2 (a) for comparison. Transparent plastic tubing (ID = 1/16 inch) was connected to the inlet and outlet of the micropump via glass tubing. HFE 7100 was used as the working fluid and the pumps were tested for the maximum pressure generation under a no flow condition.

A high voltage power supply (Trek 677 with capacity of 2 kV, accuracy  $\leq 0.1\%$  of full scale) was used with an ammeter (Keithley 2636 SourceMeter, resolution of 1 fA, accuracy better than 0.02% of reading + 25 nA) to record the current readings at different applied voltage as shown in Figure 3 (a). Static pressure head at an applied voltage was

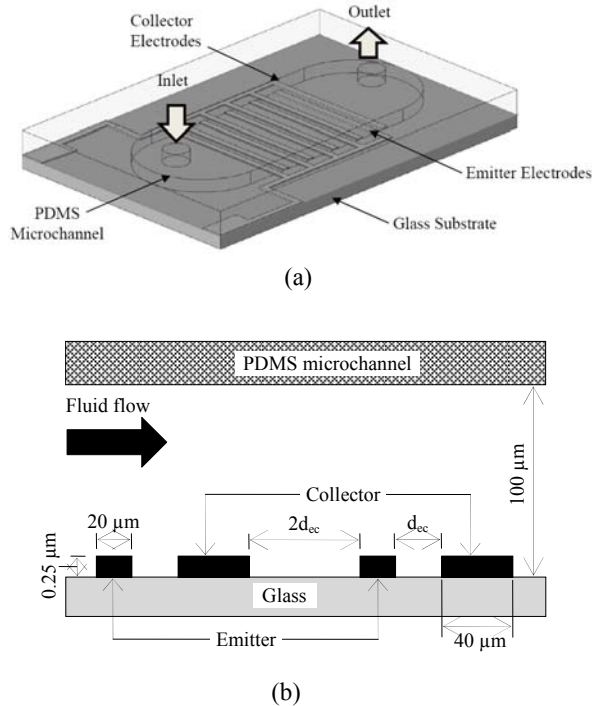


Figure 1: Schematic of (a) ion drag EHD micropump (the number of electrode pairs is 100 but only 5 pairs are shown in the schematic as a reference) and (b) dimensional specifications (not to scale).

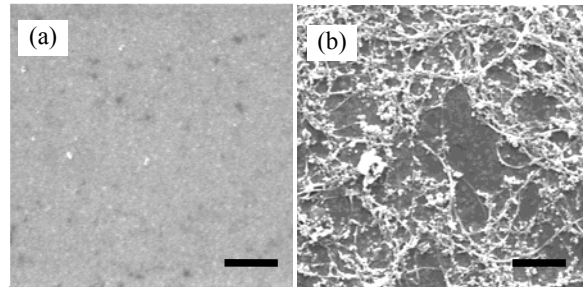


Figure 2: SEM images of electrodes (a) no deposition and (b) SWCNT deposited. Scale bar = 2  $\mu\text{m}$ .

measured from the height difference between the inlet and outlet liquid column as shown in Figure 3 (b) using a height gage (KBC tools, resolution 0.02mm).

### 3. Results and Discussion

The pumps were tested in field emission mode with a negative voltage applied to the emitter electrodes while keeping the collector

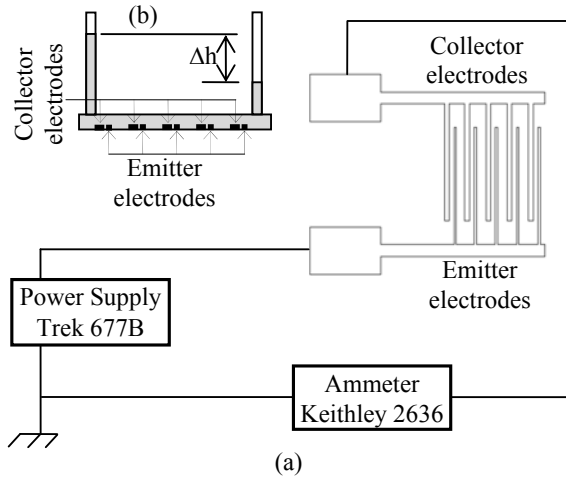


Figure 3: Schematic of the experimental facility (a) electric connections with the top view of the micropump electrodes (b) static pressure head measurement with the side view of the electrodes (the number of electrode pairs is 100 but only 5 pairs are shown in the schematic as a reference).

electrodes grounded. Operating in field emission is advantageous over field ionization due to higher charge injection and lower threshold voltage for the onset of charge injection [22, 24-27]. The discharge current for the pumps with smooth and SWCNT deposited on emitter electrodes are presented in Figure 4 at different applied voltage for the pump with inter electrode spacing of 120  $\mu\text{m}$ . The threshold voltage for the onset of charge injection, estimated as the voltage where the low slope quasi-Ohmic region intersects with

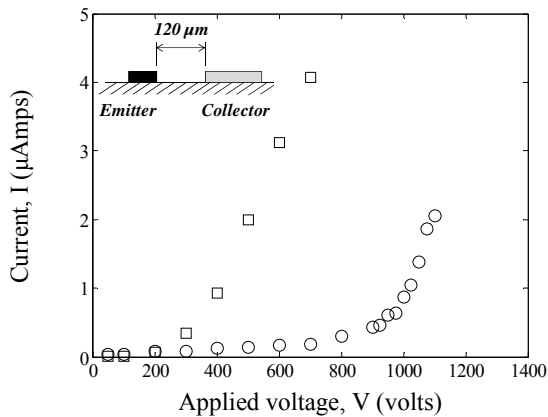


Figure 4: I-V characteristics for ○ smooth electrodes and □ SWCNT deposited on emitter electrodes for the micropump with inter electrode spacing of 120  $\mu\text{m}$ .

the steeper injection region [22], are approximately 930 and 290 V for the micropumps with smooth and SWCNT deposited on emitter electrodes respectively. The slopes of the I-V curves within the injection region were similar for both cases. A higher injection current at an applied voltage within the injection region was observed for the micropump with SWCNT compared to the one with smooth electrodes as observed previously for SWCNT or nanorods [21, 22]. This is because of the reduced work function of the electrode material due to the presence of the sharp features as found experimentally by Xue et al. [20]. An atom at the tip of a sharp structure is surrounded by fewer atoms compared to the one on a smooth surface. A higher charge density occurs at the tip of the sharp feature when a potential is applied which results in the maximum electric field at that location. Thus, when energy just above the energy barrier set by the electrode and the dielectric fluid is applied, an electron from the atoms at the tip can readily escape. On the other hand, a smooth surface is occupied by more neighboring atoms with uniformly shared free electrons which results in a comparatively stronger attraction between the electrons and the atoms. These results are consistent with those of Carvalho et al. [21] for injection in air and Russel et al. [22] for injection in HFE 7100. The reduction factor in the threshold voltage for the micropump with an inter electrode spacing of 120  $\mu\text{m}$  in this study is greater than 3. The effect of (i) the augmentation in the surface area or (ii) the decrease in the inter electrode spacing due to the introduction of the sharp features when compared to a smooth electrode, was considered by Kogut [28]. It was concluded that the presence of the sharp features with high aspect ratio had a primary effect on the charge injection enhancement while the other two parameters had a secondary effect.

The variation of the static pressure head generated at different applied voltages for the pump with smooth and SWCNT deposited on emitter electrodes are presented in Figure 5. The pressure-voltage characteristics are similar to the I-V characteristics when the two pumps

are compared. No significant pressure is generated until 900 and 500 V for the pump with smooth and SWCNT deposited on the emitter electrodes. The pressure generation at an applied voltage is greater for the pump with SWCNT deposited on the emitter electrodes. For example, the pressure generation for this pump at 1200 V is more than 5 times that of the pump with smooth electrodes. This is due to the enhancement in charge injection as seen in Figure 4; however, the enhancement in charge injection is greater than that observed in pressure generation. The generated pressure is plotted against the input power to the micropumps in Figure 6. The results show an improvement for the micropump with SWCNT

deposited on the emitter electrodes. The slope of the graph is more than 2 fold greater for the SWCNT deposited pump compared to the smooth one. The maximum pressure generation capability is also significantly improved.

Similar results were observed for the micropump with inter electrode spacing of 40  $\mu\text{m}$  and presented in Figure 7, Figure 8 and Figure 9. The pump performance is improved when the inter electrode spacing is reduced which in turns enhances the electric field. A higher current and greater pressure generation was observed for the lower inter electrode spacing. The pressure head generation within the injection region improved by a factor of

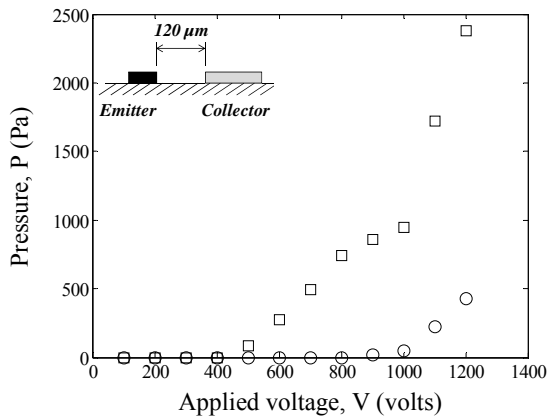


Figure 5: Static pressure generated at different applied voltage for  $\circ$  smooth electrodes and  $\square$  SWCNT deposited on emitter electrodes for the micropump with inter electrode spacing of 120  $\mu\text{m}$ .

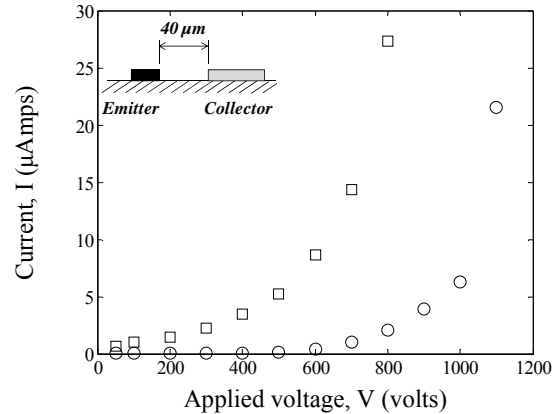


Figure 7: I-V characteristics for  $\circ$  smooth electrodes and  $\square$  SWCNT deposited on emitter electrodes for the micropump with inter electrode spacing of 40  $\mu\text{m}$ .

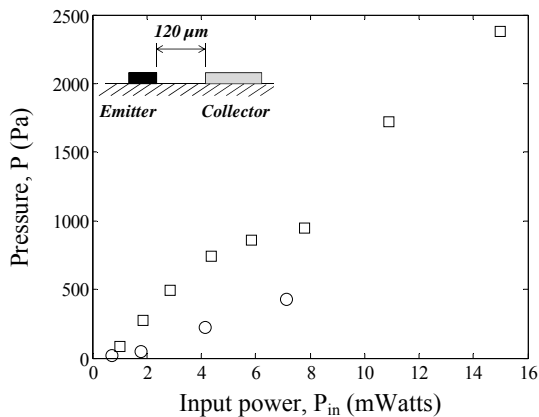


Figure 6: Static pressure generated at different input power to the pump ( $\circ$  smooth electrodes and  $\square$  SWCNT deposited on emitter electrodes) for the micropump with inter electrode spacing of 120  $\mu\text{m}$ .

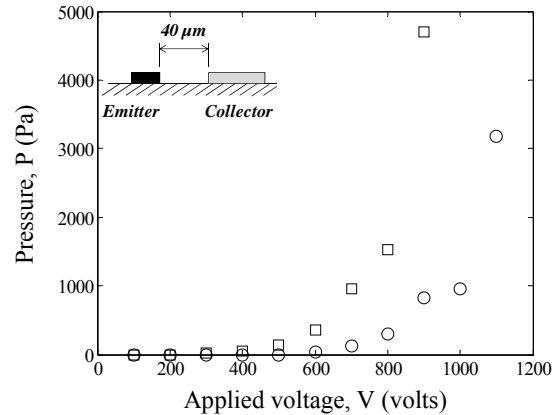


Figure 8: Static pressure generated at different applied voltage for  $\circ$  smooth electrodes and  $\square$  SWCNT deposited on emitter electrodes for the micropump with inter electrode spacing of 40  $\mu\text{m}$ .

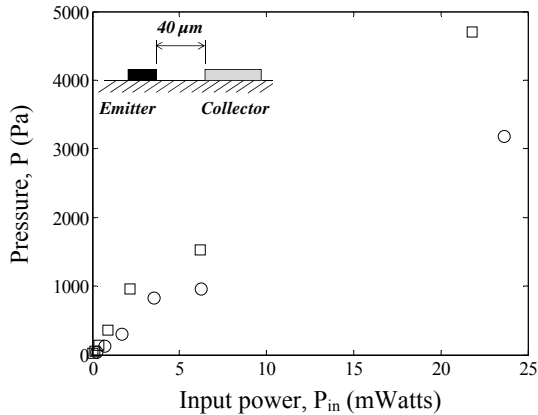


Figure 9: Static pressure generated at different input power to the pump (○ smooth electrodes and □ SWCNT deposited on emitter electrodes) for the micropump with inter electrode spacing of 40  $\mu\text{m}$ .

about 14 when the inter electrode spacing reduced from 120 to 40  $\mu\text{m}$  for the pumps with smooth electrodes (Figure 5 and Figure 8). For the pumps with SWCNT deposited on the emitter electrodes, this factor is about 5 within the injection region. The input power requirement reduces as the inter electrode spacing decreases which is consistent with the finding by Kazemi et al. [17]. The slope of the pressure-input power graph with the inter electrode spacing of 40  $\mu\text{m}$  is about twice that of the pump with inter electrode spacing of 120  $\mu\text{m}$  when the pump electrodes are smooth (Figure 6 and Figure 9). This factor is about 1.3 when SWCNT is deposited on the emitter electrodes.

#### 4. Conclusion

An experimental study was performed to determine the effect of having nano features (deposited on the emitter electrodes) on the charge injection and pressure generation of an ion drag EHD micropump using HFE 7100 as the dielectric liquid. Two micropumps were tested in this study, with and without SWCNT deposited on the emitter electrodes by electrophoretic deposition. The pumps had a total of 100 pairs of electrodes, where the width of the emitter and collector electrodes was 20 and 40  $\mu\text{m}$ , respectively. The inter electrode spacing of the two pumps were 40 and 120  $\mu\text{m}$  and the spacing between each pair

were 80 and 240  $\mu\text{m}$  respectively. The height of the microchannel was 100  $\mu\text{m}$ . Experiments were performed for a range of applied voltages across the electrode pairs. A lower threshold voltage, higher current and greater static pressure was generated for the pumps with SWCNT deposited on the emitter electrode compared to the one with smooth electrodes. A reduction factor greater than 3 in the threshold voltage was observed for the micropump with SWCNT deposited on emitter electrode when compared to the one with smooth electrodes when the inter electrode spacing was 120  $\mu\text{m}$ . This factor for the pump with inter electrode spacing of 40  $\mu\text{m}$  was about 1.4. Significant improvement in the static pressure head was observed for the pumps with both 120 and 40  $\mu\text{m}$  when SWCNT was deposited. The input power required to generate a set pressure head is lower for the pump with SWCNT deposited on the emitter electrode. The I-V or pressure-voltage characteristics suggest that the enhancement was greater for the pump with inter electrode spacing of 40  $\mu\text{m}$  compared to the one with 120  $\mu\text{m}$ . This indicates there is an optimum inter electrode spacing for achieving the best pump performance.

#### 5. Acknowledgements

The support from the Natural Sciences and Engineering Research Council of Canada (NSERC) and Canada Research Chairs Program is gratefully acknowledged.

#### 6. References

1. Mudawar, I., *Assessment of high-heat-flux thermal management schemes*. Components and Packaging Technologies, IEEE Transactions on, 2001. 24(2): p. 122-141.
2. Jiang, L., M. Wong, and Y. Zohar, *Forced convection boiling in a microchannel heat sink*. Microelectromechanical Systems, Journal of, 2001. 10(1): p. 80-87.
3. Tuckerman, D.B. and R. Pease, *High-performance heat sinking for VLSI*. Electron Device Letters, IEEE, 1981.

- 2(5): p. 126-129.
4. Iverson, B.D. and S.V. Garimella, *Recent advances in microscale pumping technologies: a review and evaluation*. *Microfluidics and Nanofluidics*, 2008. 5(2): p. 145-174.
  5. Stuetzer, O.M., *Ion Drag Pressure Generation*. *Journal of Applied Physics*, 1959. 30(7): p. 984-994.
  6. Stuetzer, O.M., *Ion Drag Pumps*. *Journal of Applied Physics*, 1960. 31(1): p. 136-146.
  7. Jorgenson, G. and E. Will, *Improved Ion Drag Pump*. *Review of Scientific Instruments*, 1962. 33: p. 55.
  8. Pickard, W.F., *Ion drag pumping. II. Experiment*. *Journal of Applied Physics*, 1963. 34(2): p. 251-258.
  9. Seyed-Yagoobi, J., J.E. Bryan, and J. Castaneda, *Theoretical analysis of ion-drag pumping*. *Industry Applications*, *IEEE Transactions on*, 1995. 31(3): p. 469-476.
  10. Richter, A., et al., *A micromachined electrohydrodynamic (EHD) pump*. *Sensors and Actuators A: Physical*, 1991. 29(2): p. 159-168.
  11. Ahn, S.-H. and Y.-K. Kim, *Fabrication and experiment of a planar micro ion drag pump*. *Sensors and Actuators A: Physical*, 1998. 70(1): p. 1-5.
  12. Crowley, J.M., G.S. Wright, and J.C. Chato, *Selecting a working fluid to increase the efficiency and flow rate of an EHD pump*. *Industry Applications*, *IEEE Transactions on*, 1990. 26(1): p. 42-49.
  13. Bryan, J. and J. Seyed-Yagoobi, *Experimental study of ion-drag pumping using various working fluids*. *Electrical Insulation*, *IEEE Transactions on*, 1991. 26(4): p. 647-655.
  14. Benetis, V., et al. *A source-integrated micropump for cooling of high heat flux electronics*. in *Semiconductor Thermal Measurement and Management Symposium, 2003. Nineteenth Annual IEEE*. 2003: IEEE.
  15. Foroughi, P., et al. *Design, testing and optimization of a micropump for cryogenic spot cooling applications*. in *Semiconductor Thermal Measurement and Management Symposium, 2005 IEEE Twenty First Annual IEEE*. 2005: IEEE.
  16. Kazemi, P.Z., P.R. Selvaganapathy, and C.Y. Ching, *Electrohydrodynamic micropumps with asymmetric electrode geometries for microscale electronics cooling*. *Dielectrics and Electrical Insulation*, *IEEE Transactions on*, 2009. 16(2): p. 483-488.
  17. Kazemi, P.Z., P.R. Selvaganapathy, and C.Y. Ching, *Effect of electrode asymmetry on performance of electrohydrodynamic micropumps*. *Microelectromechanical Systems*, *Journal of*, 2009. 18(3): p. 547-554.
  18. Zangeneh Kazemi, P., P. Ravi Selvaganapathy, and C. Ching, *Effect of micropillar electrode spacing on the performance of electrohydrodynamic micropumps*. *Journal of Electrostatics*, 2010. 68(4): p. 376-383.
  19. Darabi, J., et al., *Design, fabrication, and testing of an electrohydrodynamic ion-drag micropump*. *Microelectromechanical Systems*, *Journal of*, 2002. 11(6): p. 684-690.
  20. Xue, M., et al., *Understanding of the correlation between work function and surface morphology of metals and alloys*. *Journal of Alloys and Compounds*, 2013.
  21. Carvalho, D., et al., *Ultra-low breakdown voltage and origin of 1/f<sup>2</sup> noise in metallic nanorod arrays*. *Nanotechnology*, 2008. 19(44): p. 445713.
  22. Russel, M.K., Selvaganapathy, P.R., Ching, C.Y., *Effect of electrode surface topology on charge injection characteristics in dielectric liquids: an experimental study*. *Journal of Electrostatics (Submitted)*, 2014.
  23. Gao, B., et al., *Fabrication and electron field emission properties of carbon nanotube films by electrophoretic deposition*. *Advanced*

- materials, 2001. 13(23): p. 1770-1773.
24. Butcher, M., et al., *Conduction and breakdown mechanisms in transformer oil*. Plasma Science, IEEE Transactions on, 2006. 34(2): p. 467-475.
  25. Schmidt, W.F., *Electronic conduction processes in dielectric liquids*. Electrical Insulation, IEEE Transactions on, 1984(5): p. 389-418.
  26. Halpern, B. and R. Gomer, *Field emission in liquids*. The Journal of Chemical Physics, 2003. 51(3): p. 1031-1047.
  27. Halpern, B. and R. Gomer, *Field ionization in liquids*. The Journal of Chemical Physics, 2003. 51(3): p. 1048-1056.
  28. Kogut, L., *The influence of surface topography on the electromechanical characteristics of parallel-plate MEMS capacitors*. Journal of Micromechanics and Microengineering, 2005. 15(5): p. 1068.